

SMA memo 148

Noise Characterization and Allan Variances of Water Vapor Monitors

Martina C. Wiedner, June 2002

1. Abstract

The noise performance of the Sub-Millimeter Array radiometers has been investigated with on site measurements in July 2000. The instrumental set-up, the measurements and the data analysis using the Allan variance method are presented in this memo. The measurements show that the performance of the instrument is limited, as expected, by the mixer and the first stage amplifier rather than components later in the detection chain. The noise is dominated by thermal noise (“White (Frequency) Noise”) on time scales below a few seconds, but by gain variations (“Flicker (Frequency) Noise”, “Random Walk of (Frequency) Noise”) on larger times scales. The Allan variance hence shows that the lowest noise on any measurement can be obtained by averaging measurements over a few seconds and by re-calibrating the gain every ~ 10 or 20 s.

2. Introduction to Water Vapor Monitors

The Water Vapor Monitors are build to allow interferometric phase correction by monitoring the sky brightness temperature in three double sideband frequency channels in the wing of the 183.3 GHz water vapor line, see Fig. 1. Channel 1 is 1.2 GHz away from the line center and covers about 181.9 - 182.3 GHz and 184.3 - 184.7 GHz, channel 2 is 4.2 GHz away from the line center and covers about 178.6 -179.6 GHz and 187.0 - 188 GHz, and channel 3 is 7.8 GHz away from the line center covering about 175.0 - 176.0 GHz and 190.6 - 191.6 GHz. Two such radiometers are currently installed on the Sub-Millimeter Array (SMA) to test this method of phase correction. The radiometers employ a room temperature subharmonic Schottky diode mixer and have system temperatures of 1800 to 2500 K. In order to correct the interferometric phase effectively, it is essential to reduce the instrumental noise of the radiometers to about 10^{-4} of the total detected power. (For phase correction to $\sim 30^\circ$ at 350 GHz, we need to detect changes in the optical paths of $\sim 80\mu\text{m}$, which is equivalent to changes in the total water column of $\sim 13\mu\text{m}$, or brightness temperature changes of about 0.3 K.) In order to achieve this accuracy gain changes of the amplifier and the mixer are measured on two internal calibration loads at about 30°C (303 K) and 100°C (373 K). The data presented below were taken with the WVM originally build for the Caltech Submillimeter Observatory (CSO).

3. Allan variance

The radiometers allow measurements in all three channels each second: They integrate 0.2 s on the hot load, 0.2 s on the warm load and 0.4 s on the sky. The Allan variances of the hot and the warm load measurements were calculated for each channel assuming that the load brightness temperature is constant.

The Allan variance is basically an average of the mean square deviations from two adjacent samples. In contrast to the variance it follows level changes in the data (for

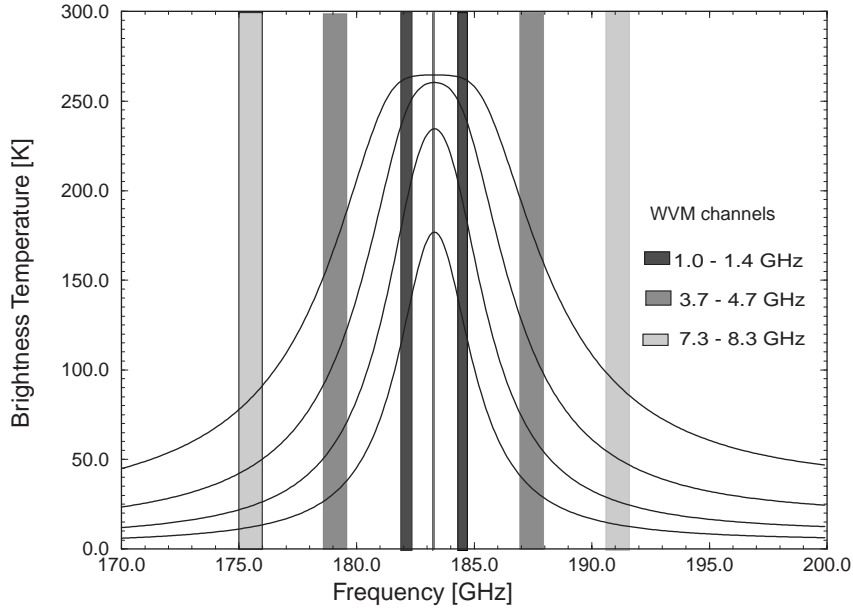


Figure 1. Passbands of the three double-sideband WVM channels.

an explanation see Thompson, Moran and Swenson, 2001) and is therefore a powerful analysis tool for noise that is not purely Gaussian, e.g. for $1/f$ noise. For data sampled at time interval Δt , the Allan variance is simply the deviation of $y(j)$ from the line connecting $y(j-1)$ and $y(j+1)$:

$$\text{Allan variance} = \frac{1}{N-2} \sum_{j=2}^{N-1} \left(\frac{y(j-1) + y(j+1)}{2} - y(j) \right)^2 \quad (1)$$

This is the Allan variance of $\tau = 1 \times \Delta t$. Then bins containing 2 data points each are formed and the Allan variance is calculated in the same way, etc., i.e. for $\tau = k \times \Delta t$:

$$y(j) = \frac{1}{k} \sum_{i=j+1}^{j+k} x(i) \quad (2)$$

where $x(i)$ is the i th data point of variable x , e.g., the i th measurement of the hot load in channel 1. The Allan standard deviation is the square root of the Allan variance. In the program used here the Allan variance is normalized by dividing by the average squared, so that the receiver temperature and detection level are divided out and the Allan variances can be directly compared.

If the noise on the data is uncorrelated, the Allan variance is $3/2$ times the variance ($3/2$ times the rms squared). (To prove this write down the expressions for rms and Allan variance using $x(i) = \bar{x} + \delta(i)$ with $\sum \delta(i) = 0$ and $\sum \delta(i)\delta(i+1) = 0$.)

The different slopes of the Allan variance plotted against tau in a log-log plot reflect the different types of noise. Thompson et al. (2001) have discussed the Allan variance using a frequency standard as an example. Similar noises are seen with the radiometers.

1. **White Phase Noise** and **Flicker Phase Noise** have a slope of -2 in the Allan variance (-1 in the Allan standard deviation). The former is expected to be additive noise in amplifiers, the latter in transistors. These noises dominate at very short integration times and are not seen in our data.
2. **White (Frequency) Noise** or **Random Walk of Phase Noise** have a slope of -1 in the Allan variance (-1/2 in the Allan standard deviation). They are due to additive noise such as thermal noise. Its value can be calculated with $\frac{3}{2} \frac{T_{Rx} + T_{signal}}{\Delta\nu \Delta\tau}$, where $\Delta\nu$ is the bandwidth of the filter and $\Delta\tau$ the integration time. In our case we plotted the normalized Allan variance, which means that $T_{Rx} + T_{signal}$ was divided out and the noise simply depends on integration time and filter bandwidth $\frac{3}{2} \frac{1}{\Delta\nu \Delta\tau}$. This type of noise is clearly seen in our data and we refer to it as “thermal noise”.
3. **Flicker (Frequency) Noise** has a slope of 0 in both the Allan variance and the Allan standard deviation.
4. **Random Walk of (Frequency) Noise** has a slope of +1 in the Allan variance (+1/2 in the Allan standard deviation). This noise is sometimes also called the “1/f Noise”. Similar to the Flicker (Frequency) Noise it is assumed to arise from random changes in temperature, pressure or magnetic field in the instrument. These two noises are associated with long term drifts. We see them clearly in our measurements and refer to them as “gain variations”. They can be corrected for by calibrating the instrument in time intervals shorter than the time scale of the drifts.

4. Data and Results

In order to calculate the theoretical thermal noise, the filter bandwidths were measured and are plotted in Fig. 2. The filter width is defined as the width between the 3dB points.

- Filter 1 215 MHz
- Filter 2 450 MHz
- Filter 3 505 MHz

(The total passband of each channel is 4 times the filter width because the instrument has two down conversions both of which are double sideband, see Fig. 6.)

A detailed summary of the set-up for each Allan variance measurement is given in Table 1 and sketched in the even numbered figures 4 - 24, whereas the data is shown in the odd numbered figures 3 - 23. The described experiments were performed in July 2000 in the CSO receiver lab (on the summit) and on the CSO telescope. The first three experiments described here (v2f, 001 and 002) were performed on the 12th of July, experiment 005 and 006 on the 13th July and the rest on the 14th of July 2000.

We discuss the results and conclusion from each data set as follows:

- **Voltage to Frequency converters and backend (v2f, Fig. 3)**

Set-up: A 5 V power supply is split and connected to all 3 Voltage to Frequency converters (V/F). The WVM computer reads out the counts from the V/Fs.

Discussion: The Allan variance on the Voltage to Frequency Converters (V/F) and computer lies below 10^{-10} , slightly lower for channel 1, but in all cases much lower than the Allan variance of the entire system (10^{-8} for $\tau = 1$). The expected value of the Allan variance at $\tau = 1$ is -10.4. (The counter will roughly get

200000 counts a second, and has an accuracy of 1 count, the error should hence be $1/200000$ and the Allan variance $\log_{10}((3/2) * (1/(200000))^2) = -10.4$.) The Allan variance has a slope of -1 until 4 sec, then the Allan variance flattens and increases after approximately 40 sec. Since it has the same slope in all 3 channels it is most likely that there are output variations in the 5V power supply. In all Allan variance plots, the noise of the Allan variance increases with τ . For $\tau > 100$ oscillations are often seen. Since we are not interested in the exact values of the Allan variance at these long integration times (large τ), no attempt as been made to suppress the oscillations by filtering the data or other techniques.

Conclusion: *The noise of the V/F and computer are insignificantly smaller than the noise of the overall system and neither the V/Fs nor the counters will degrade the signal noticeably.*

- **Normal set-up (allan001, Fig. 5)**

Set-up: The WVM was set-up as it would normally operate with the exception that this data was taken in the lab.

Discussion: The Allan variance decreases with a slope of -1 between 1 and about 5 sec. The slope as well as the value agree very well with theoretical calculations of thermal noise (straight line in plots on the right). Around 10 to 30 seconds the Allan variance has a minimum and the noise increases for $\tau > 30$ sec. The Allan variance of channel 3 is lower than that of channel 2 by $10^{0.15}$, but the expected difference - due to the narrower filter of 450 MHz versus 505 MHz - is only $10^{0.05}$.

Conclusion: *The WVM shows the expected thermal noise between about 1 and 5 seconds. On time scales larger than 5 s gain variations are noticeable and they dominate for time scales larger than 30 s. It is important to calibrate the WVM every ~ 5 sec.*

- **Exchanging detector 2 and 3 (002, Fig. 7)**

Set-up: The 4.2 GHz signal is input into detector and V/F of channel 3 and the 7.8 GHz signal into that of detector and V/F of channel 2.

Discussion: The Allan variance looks very similar. At a closer look, the Allan variance of the warm and hot load of individual channels overlap better. The Allan variance in the channel that includes detector 2 is higher by $10^{0.2}$ than of that including detector 3. A difference of Allan variance of $10^{0.2}$ suggests a bandwidth (or integration time) difference of 60%, e.g. 320 MHz and 505 MHz filter bandwidth. It is unclear what might cause this $10^{0.2}$ (rather than $10^{0.05}$) difference in Allan variance, as the same detector boxes plus V/Fs were used to measure the bandwidth. (i.e. if the amplifier in the detector box limits the bandwidth, it should already be included in the measurement of the bandwidth.) The 1/f noise is not very correlated between the channels.

Conclusion: *The detector and V/F of channel 2 and 3 have comparable noise.*

- **Exchanging different components of channels 2 and 3 (002, 005, 006, Fig. 7, 9, 11)**

This is a summary of the three experiments in which different components of channel 2 and 3 were exchanged.

1. Channel 1
 - $10^{0.1}$ above theoretical Allan variance at 1sec
 - thermal behavior only until 2.5 s ($10^{0.4}$). For longer time scales gain variations become noticeable and dominate for times larger than 25 s.
2. The differences in value and slope of Allan variance in channel 2 and 3 seem to depend on the detector box alone.

3. Detector 2

- Allan variance $10^{0.1}$ above theoretical value
- Thermal noise dominates until 3 s ($10^{0.5}$ s).

4. Detector 3

- The Allan variance agrees with theory at 1sec.
- The thermal noise is dominant until 5 s ($10^{0.7}$ s).
- Detector 3 (det3) seems better. Note that det3 has a slightly wider filter (which is expected to decrease the noise by $10^{0.05}$. However, we see a decrease by $\sim 10^{0.15}$.)

5. Filter width

From the measured Allan variances at $\tau=1$ we can calculate the filter bandwidths under the assumption of the predominance of thermal noise and an integration time of 0.2 s:

- Channel 1 150 MHz (cf. 215 MHz)
- Channel 2 375 MHz (cf. 450 MHz)
- Channel 3 530 MHz (cf. 505 MHz)

This might indicate that the noise is not purely thermal even at 1 s. Alternatively, there might be other bandwidth limiting components or the integration time might be shorter than programmed (the latter is very unlikely).

Conclusion: *Except for small deviations, all components perform as expected.*

- **Exchanging components of channel 1 and 3 (007 and 008, Fig. 13,15)**

This is a summary of the two experiments in which different components of channel 1 and 3 were exchanged.

Set-up: Since detector and V/F of channel 3 have slightly less noise than channel 2, we swapped channel 1 and 3 (rather than 2). In 007 the 1.2 GHz input was connected to detector and V/F of channel 3, in 008 only the detectors 1 and 3 exchanged, but not the V/Fs.

Discussion: The theoretical and the measured Allan variance do not agree in the bottom plot of Fig. 13 nor the top plot of Fig. 15. In both cases the 1-2 GHz IF is mixed with 1.2 GHz and fed into detector 3 that has a 505 MHz wide filter. However the IF is not wide enough for this filter. Only the signal between 1.0 and 1.7 GHz will be detected (assuming the amplifier has a sharp cut-off below 1 GHz). The effective bandwidth is therefore 700 MHz/2, which gives an expected Allan variance of $10^{-7.7}$. This agrees well with the data.

Conclusion: *Detector and V/F of channel 1 work fine and are similar to those of channel 3 when taking the difference in filter band width into account.*

- **Monochromatic wave (1.3 GHz, -14 dBm) from signal generator in channel 1 (009, Fig. 17)**

Set-up: So far all experiments were devised to check detectors and V/F of different channels, but the gain fluctuations seemed unaffected by any changes in the backend. It is possible that the gain variations of the Schottky mixer and/or of the first and/or second amplifier are dominant at short time scales (~ 5 s). Therefore a set-up was devised that excludes these three components: A monochromatic wave at 1.3 GHz (-14 dBm) is input into the second down converter of channel 1. The signal level is chosen so that the output level of the WVM is the same as with the normal set-up. After down converting with the 1.2 GHz oscillator the IF is sent to detector and V/F of channel 3 because these performed best earlier.

The signal generator had been switched on for ~ 30 min before the measurement, i.e., the signal could still be drifting due to the generator warming up.

Discussion: The gain fluctuations become significant at $10^{0.3} = 2$ seconds. The Allan variance does not show the -1 slope typical for thermal noise and is lower than in the other two channels. This is due to the receiver temperature being very small compared to the gain variations in this set-up.

The shape of the Allan variance seems to indicate that there are fast gain variations (~ 2 s) not seen in the entire system. These gain variations might be caused by the signal source.

Conclusion: *The Schottky mixer, first and/or second amplifier contribute most to the receiver temperature.*

- **Monochromatic wave (1.3 GHz, -45 dBm) from signal generator input in channel 1 before amplifier (010, Fig. 19)**

Set-up: In order to investigate the contribution of the second amplifier, the signal generator was connected to the second amplifier. Schottky mixer and the first amplifier were not used in this set-up. To obtain the same output level the monochromatic signal at 1.3 GHz was decreased to -45 dBm.

Discussion:

1. For small τ the Allan variance is larger than in the previous set-up, but smaller than in the standard radiometer set-up. This must be due to the receiver noise from the second amplifier being larger than the noise from second down converters, V/Fs, detectors and counters, but smaller than the noise from mixer and first amplifier.
2. The Allan variance has a slope of -1 for times shorter than 6 s. The thermal noise dominates over gain variations at these short time scales.
3. The gain fluctuations presumably of the second amplifier only become significant at $10^{0.8} = 6$ seconds, i.e. the second amplifier seems to have slower gain variations than the complete system.

Conclusion: *For a set-up without the Schottky mixer and without the first amplifier, the second amplifier is the dominant cause of the receiver temperature. The gain variations of the second amplifier are slower than those of the Schottky mixer and or first amplifier.*

- **Normal set-up on telescope (019, Fig. 21)**

Set-up: The WVM was put back into its original state and mounted on the CSO telescope. A bucket of liquid nitrogen was put in front of the radiometer, so that the sky channel sees the liquid nitrogen. The CSO telescope was not moving.

Discussion:

1. The additional black lines in Fig. 21 are the Allan variances of the sky channel. Since the integration on the sky is twice as long, the Allan variance is expected to be lower by a factor of 2 (lower by 0.3 on a logarithmic scale). This agrees with the measurement as long as the noise is dominated by thermal noise.
2. The Allan variance of the WVM on the telescope looks very similar to those measured inside the lab, suggesting that no noise is added, at least if the telescope is not moving.

Conclusion: *No noise is added by the WVM being mounted on the telescope, neither due to thermal instabilities nor due to interference.*

- **Normal set-up on moving telescope (011, Fig. 23)**

Set-up: The WVM was put back into its original state and mounted on the CSO telescope. The CSO telescope and the WVM were tipping in elevation.

Discussion: The Allan variances are very similar to the ones in 019.

Conclusion: *Neither the thermal noise nor the gain variations increase when the telescope and the WVM are tipping.*

5. Conclusion

1. The noise contribution/error due to quantization of the voltage to frequency converters is insignificant in comparison to the noise due the front end.
2. The instrument is dominated by thermal noise from the subharmonic mixer and the first amplifier, which are also responsible for some, but not all of the gain fluctuations.
3. The electrical components perform as expected, none have any obvious faults.
4. The measured Allan variance is sometimes slightly higher than expected. However, the measured noise (square root of Allan variance) is never more than 25% above the expectation. The system seems to perform more or less as expected.
5. The WVM is dominated by thermal noise up to time scales of a few seconds when gain fluctuations (“Flicker (Frequency) Noise” and the “Random Walk of (Frequency) Noise”) become significant.
 - This underlines the need for calibration on time scales of a few seconds, but it is not necessary to calibrate more frequently.
 - Hot load, warm load or sky should not be smoothed over more than a few seconds. (However, the system temperature, can be smoothed over longer times.)
6. The gain fluctuations have the expected slopes of 0 for the “one-over-f noise” between about 10 and 30 s, and the expected slope of 1 for “flicker frequency noise” for longer time scales. The gain fluctuations are very well correlated within a channel, but appear to correlate poorly between the different channels on long time scales (>100s). This suggests that the components that are channel specific dominate the gain fluctuations on long time scales. It is most probable that the mixer and the first amplifier dominate the fast fluctuations.

→ **As expected the mixer and the first amplifier limit the performance of the WVMs. Most of the thermal noise and possibly quite a lot of the gain fluctuations (“Flicker (Frequency) Noise” and the “Random Walk of (Frequency) Noise”) are caused by the mixer and the first amplifier. No single component in the backend is noticeably worse than the others.**

→ **The accuracy of the measurement is limited by gain fluctuations, therefore frequent calibration is essential. Future instruments should allow for frequent calibration and/or be more stable and/or have lower receiver temperatures.**

6. Future Measurements

Here are some suggestions for future measurements:

1. The V/F performance could be determined to higher accuracy by using a 5V battery supply, which will have much smaller gain drifts than the power supply. (For the discussion above the crucial point is that the V/F noise is negligible in

comparison to the noise of the front end, but for a different low noise front end such a measurement might be very interesting.)

2. Another attempt of measuring the Allan variance of the first and second amplifier and the second down-converter could be made. The main difficulty is that the gain variations of the input as well as that of the backend have to be insignificant in comparison to the device studied. It was suggested that a cooled amplifier with a resistive load is a very stable noise source, which could be used as the input of the first and second amplifier. Since the existing backend is well characterized it might be possible to use it.
3. Similar measurements could be performed on the second radiometer operated at the SMA, which was built by the Herzberg Institute of Astronomy.

7. Acknowledgments

I would like to thank David Wood who gave me the idea to study the Allan variance of the 183 GHz WVM. Further I am grateful to the CSO for letting me use their lab and equipment for these tests, and the CSO staff for their patience and tolerance with me. I would like to thank Ray Blundell, Ed Tong and Hugh Gibson for the suggestions for future measurements. Jim Moran and James Battat carefully read through the manuscript and made very helpful suggestions to improve the document.

8. References

Thompson, A. R., Moran, J. M., & Swenson, G. W. 2001, *Interferometry and Synthesis in Radio Astronomy* (2nd ed.; New York, NY: John Wiley & Sons), p. 334

File	Samples	Experiment	Figure
v2f	900	5V input in all V/F's,	Fig. 3, 4
001	1800	WVM in lab, normal set-up	Fig. 5, 6
002	1800	WVM in lab, lid open	Fig. 7, 8
		1.2 GHz det1 V/F1 counter 1	
		4.2 GHz 0dB det3 V/F3 3	
		7.8 GHz 6 det2 V/F2 2	
005	3600	WVM in lab, lid open	Fig. 9, 10
		1.2GHz dB det1 V/F 1 counter 1	
		4.2GHz 0dB 3 2 2	
		7.8 6 2 3 3	
		offsets det1=0.1 kHz, det2=-2 kHz (?), det3=0.7 kHz	
006	3600	WVM in lab, lid open	Fig. 11, 12
		1.2GHz dB det1 V/F 1 counter 1	
		4.2GHz 1dB 2 V/F 3 3	
		7.8GHz 6dB 3 V/F 2 2	
007	3600	WVM in lab, lid open	Fig. 13, 14
		1.2GHz 6dB det3 V/F 3 counter 3	
		4.2GHz 1dB 2 2 2	
		7.8GHz 0dB 1 1 1	
008	3600	WVM in lab, lid open	Fig. 15, 16
		1.2GHz 6dB det3 V/F1 counter 1	
		4.2GHz 1dB 2 2 2	
		7.8GHz 0dB 1 3 3	
009	3600	WVM in lab, lid open	Fig. 17, 18
		Signal source input @-14dBm at 1.3GHz aftersecond amplifier, but before mixer.	
		1.3GHz 6dB det3 V/F3 counter 3	
		4.2GHz 1dB 2 2 2	
		7.8GHz 0dB 1 1 1	
010	3600	WVM in lab, lid open	Fig. 19, 20
		Signal source input @ -45dBm at 1.3GHz before second amplifier, and before mixer. Signal level is chosen so that the output of the WVM is always ~900 kHz. Signal generator had been switched on for ~100 min before measurement, should be stable.	
		1.3GHz 6dB det3 V/F 3 counter 3	
		4.2GHz 1dB 2 2 2	
		7.8GHz 0dB 1 1 1	
019	3600	WVM on CSO telescope looking at liquid N ₂	Fig. 21, 22
		1.3GHz 0dB det1 V/F 1 counter 1	
		4.2GHz 1dB 2 2 2	
		7.8GHz 6dB 3 3 3	
011	3600	WVM on CSO, WVM looking at sky,CSO tipping	Fig. 23, 24
		1.3GHz 0dB det1 V/F 1 counter 1	
		4.2GHz 1dB 2 2 2	
		7.8GHz 6dB 3 3 3	

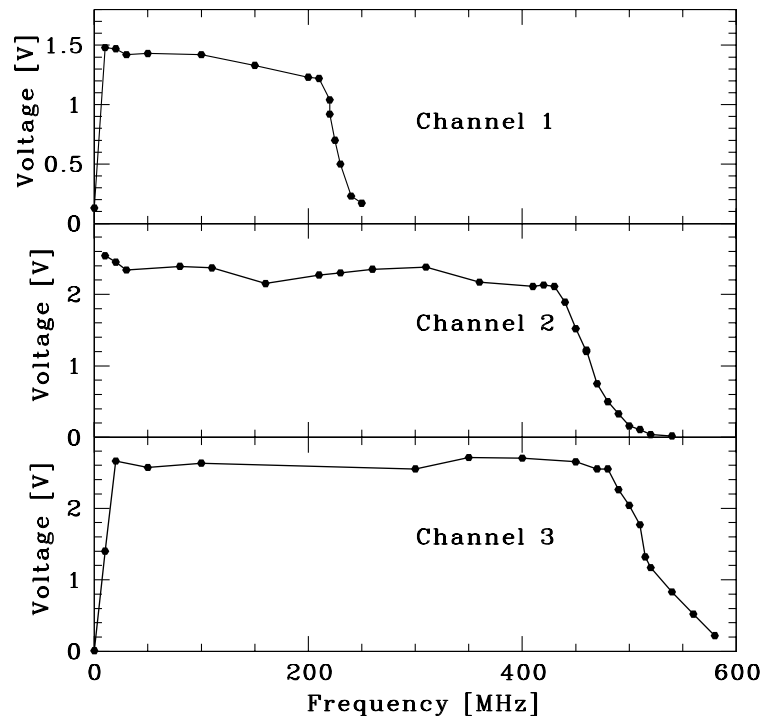


Figure 2. Low pass filters of WVM. Channel 1 has a band width of 215 MHz, Channel 2 of 450 MHz, and Channel 3 of 505 MHz.

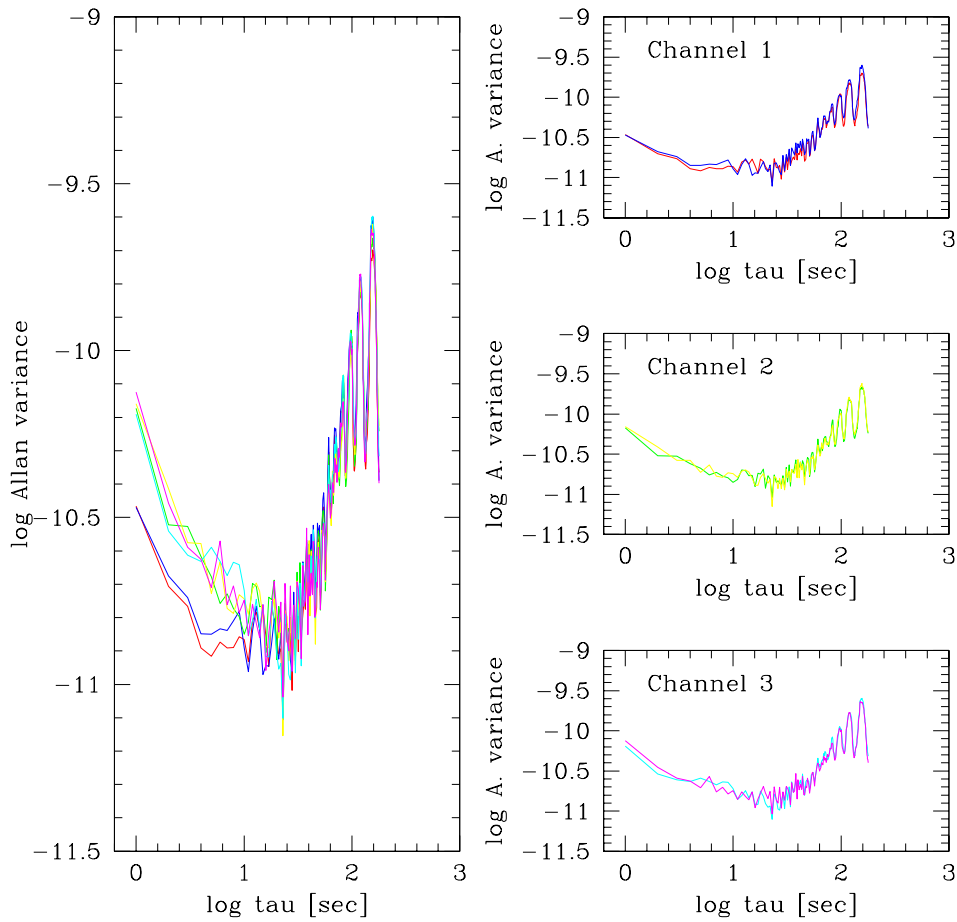


Figure 3. Allan variance of the V to F converters. Channel 1 hot: red, warm: blue. Channel 2 hot: yellow, warm: green. Channel 3 hot: magenta, warm: turquoise.

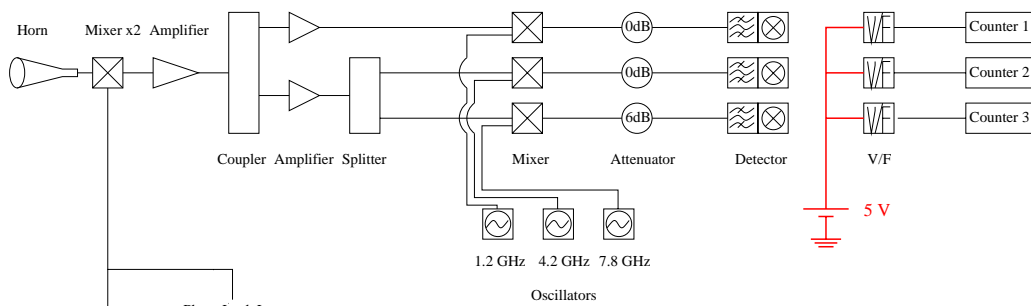


Figure 4. Set-up for the Allan variance plotted above. A power supply is directly connected to the V/Fs and the counters, the rest of the radiometer is not used.

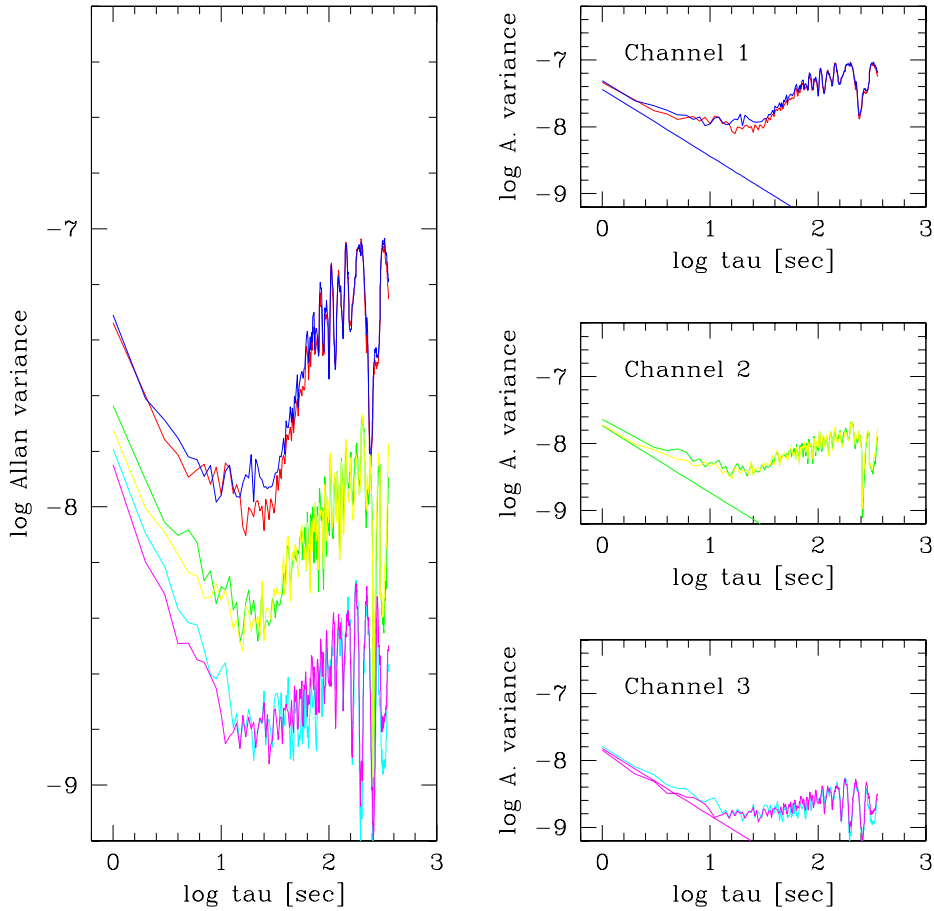


Figure 5. Allan variances of hot and warm loads of channels 1 to 3 for the set-up depicted below, also see table file 001. Channel 1 hot: red, warm: blue. Channel 2 hot: yellow, warm: green. Channel 3 hot: magenta, warm: turquoise. The channel number is defined by the counter, not by the input frequency. The straight lines are the theoretical expectations for thermal noise alone. The panel on the left shows all data combined, the three panels on the right are channels 1, 2 and 3 from top to bottom.

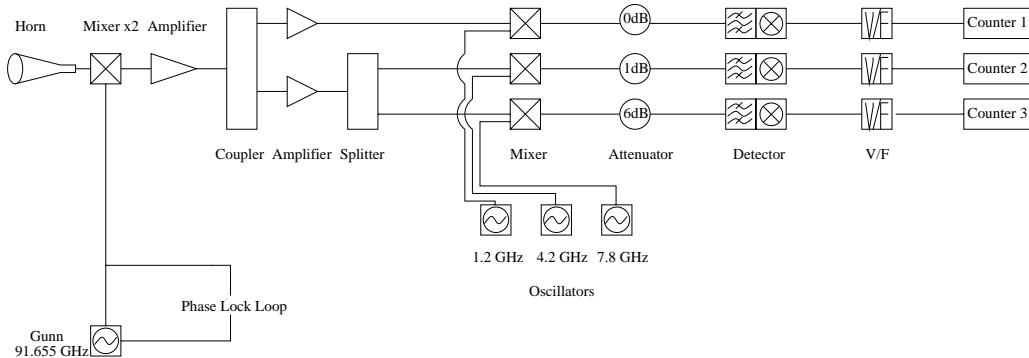


Figure 6. Set-up for Allan variances plotted above (file 001).

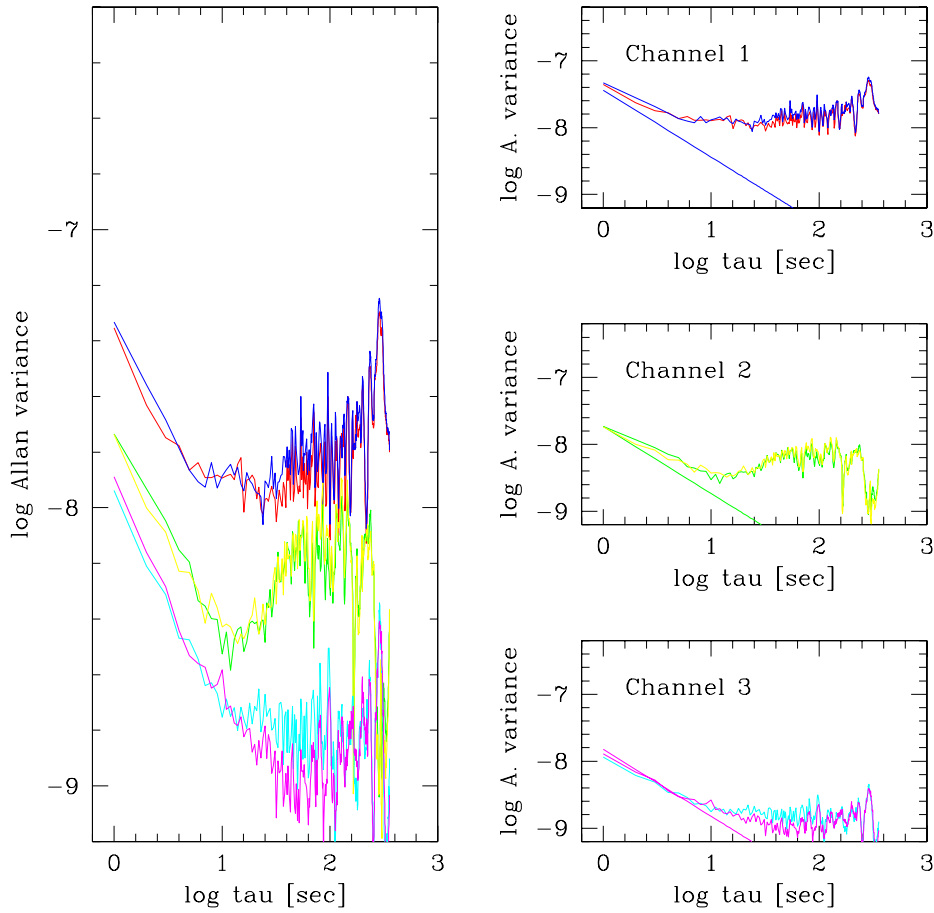


Figure 7. Allan variances of hot and warm loads of channels 1 to 3 for the setup depicted below, also see description for file 002 in table. Channel 1 hot: red, warm: blue. Channel 2 hot: yellow, warm: green. Channel 3 hot: magenta, warm: turquoise. The channel number is defined by the counter, not by the input frequency. The straight lines are the theoretical expectations for thermal noise alone.

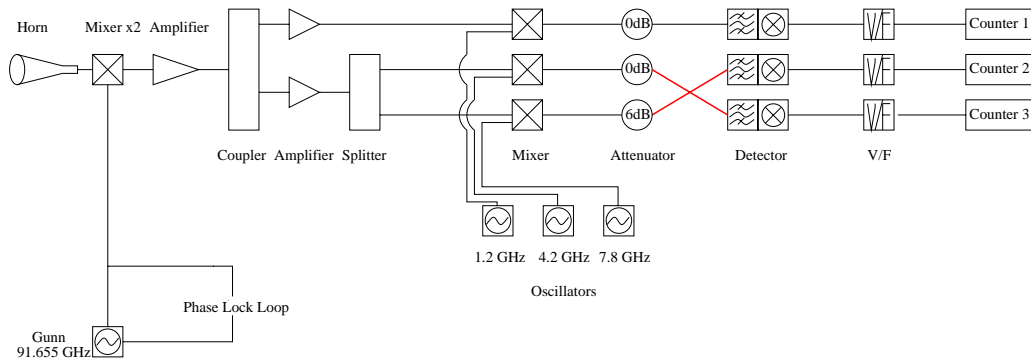


Figure 8. Set-up for Allan variances plotted above (file 002).

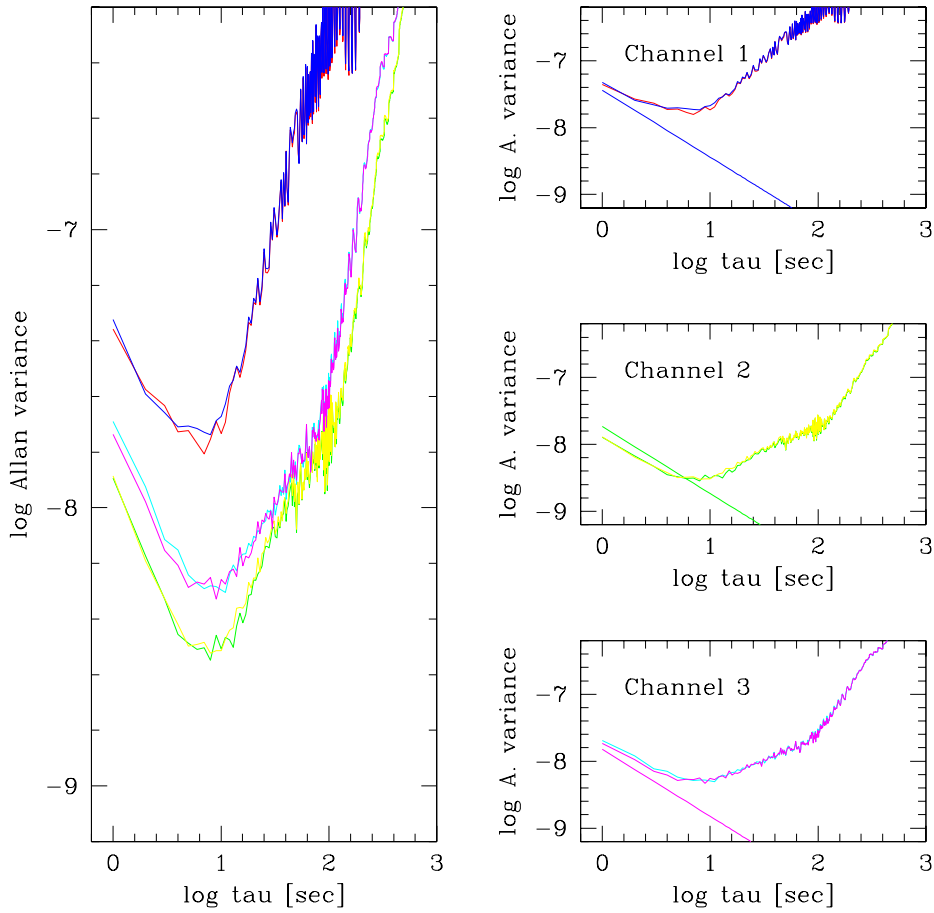


Figure 9. Allan variances of hot and warm loads of channels 1 to 3 for the setup depicted below, also see description for file 005 in table. Channel 1 hot: red, warm: blue. Channel 2 hot: yellow, warm: green. Channel 3 hot: magenta, warm: turquoise. The channel number is defined by the counter, not by the input frequency. The straight lines are the theoretical expectations for thermal noise alone.

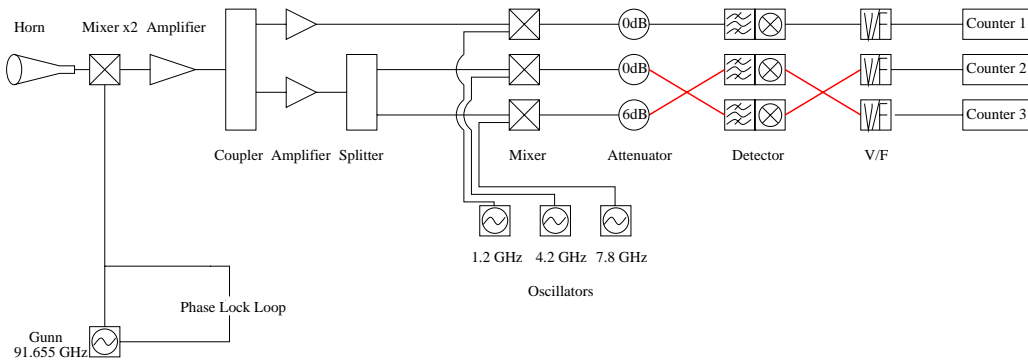


Figure 10. Set-up for Allan variances plotted above (file 005).

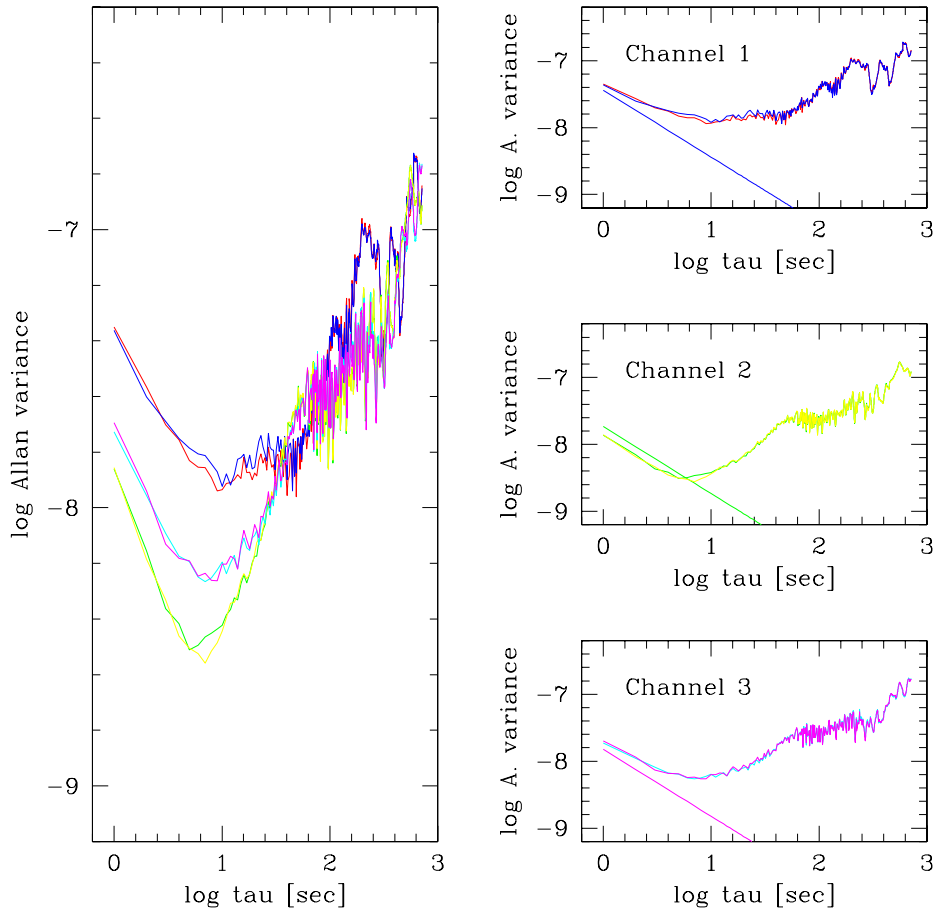


Figure 11. Allan variances of hot and warm loads of channels 1 to 3 for the setup depicted below, also see description for file 006 in table. Channel 1 hot: red, warm: blue. Channel 2 hot: yellow, warm: green. Channel 3 hot: magenta, warm: turquoise. The channel number is defined by the counter, not by the input frequency. The straight lines are the theoretical expectations for thermal noise alone.

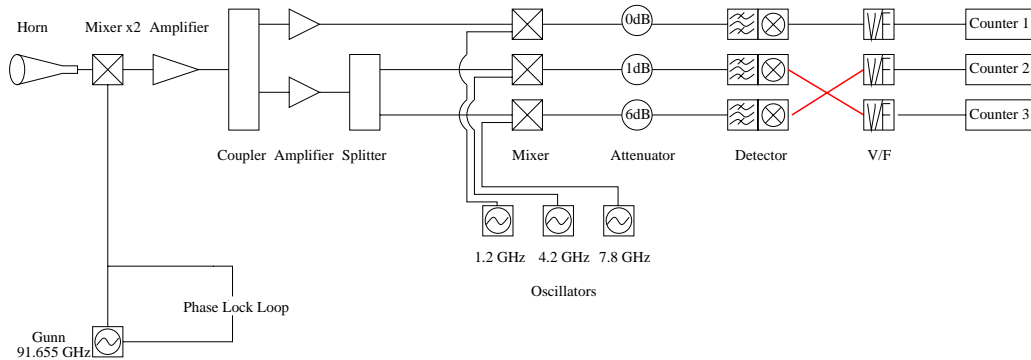


Figure 12. Set-up for Allan variances plotted above (file 006).

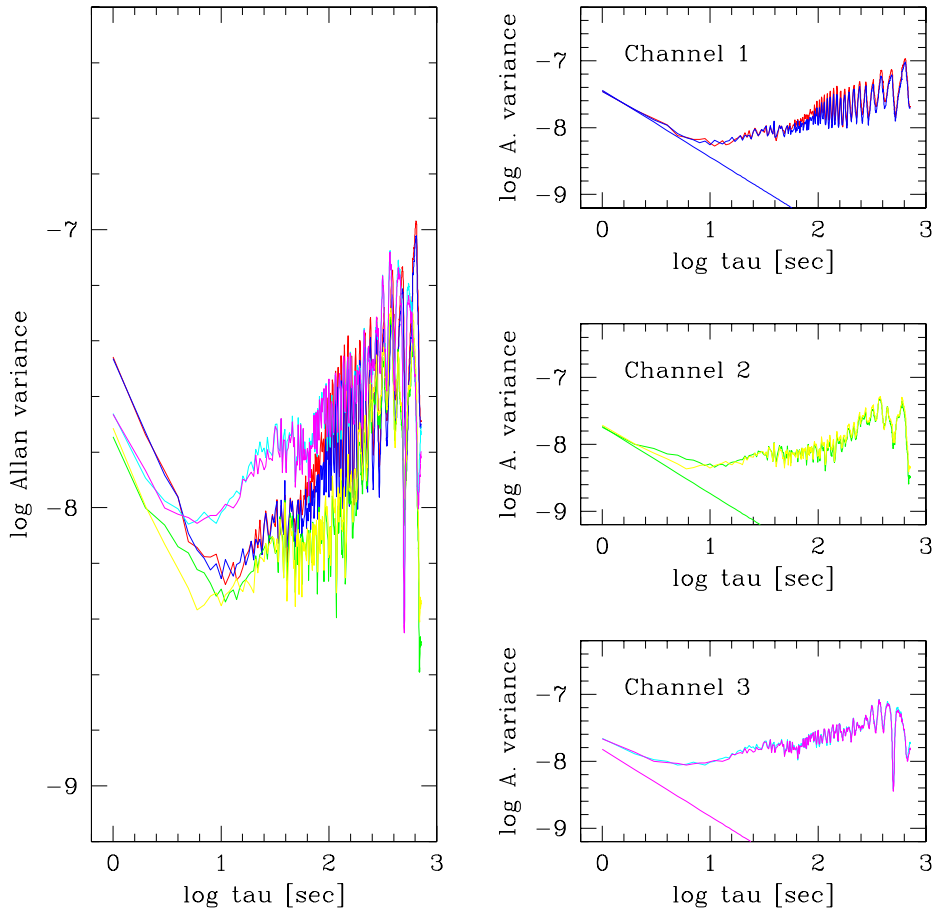


Figure 13. Allan variances of hot and warm loads of channels 1 to 3 for the setup depicted below, also see description for file 007 in table. Channel 1 hot: red, warm: blue. Channel 2 hot: yellow, warm: green. Channel 3 hot: magenta, warm: turquoise. The channel number is defined by the counter, not by the input frequency. The straight lines are the theoretical expectations for thermal noise alone.

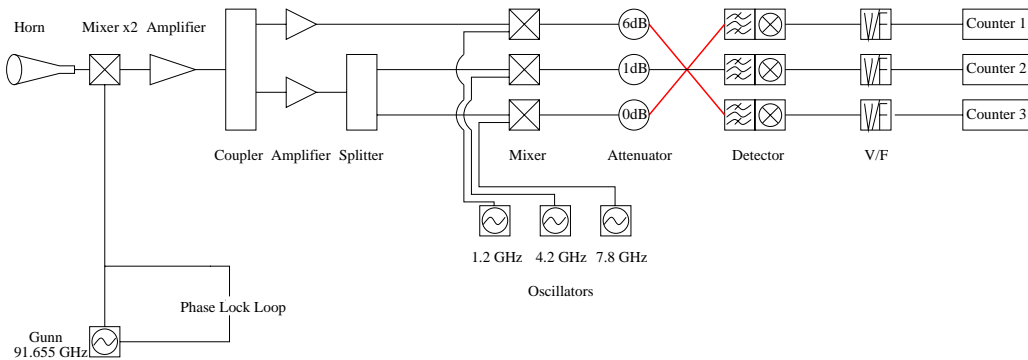


Figure 14. Set-up for Allan variances plotted above (file 007).

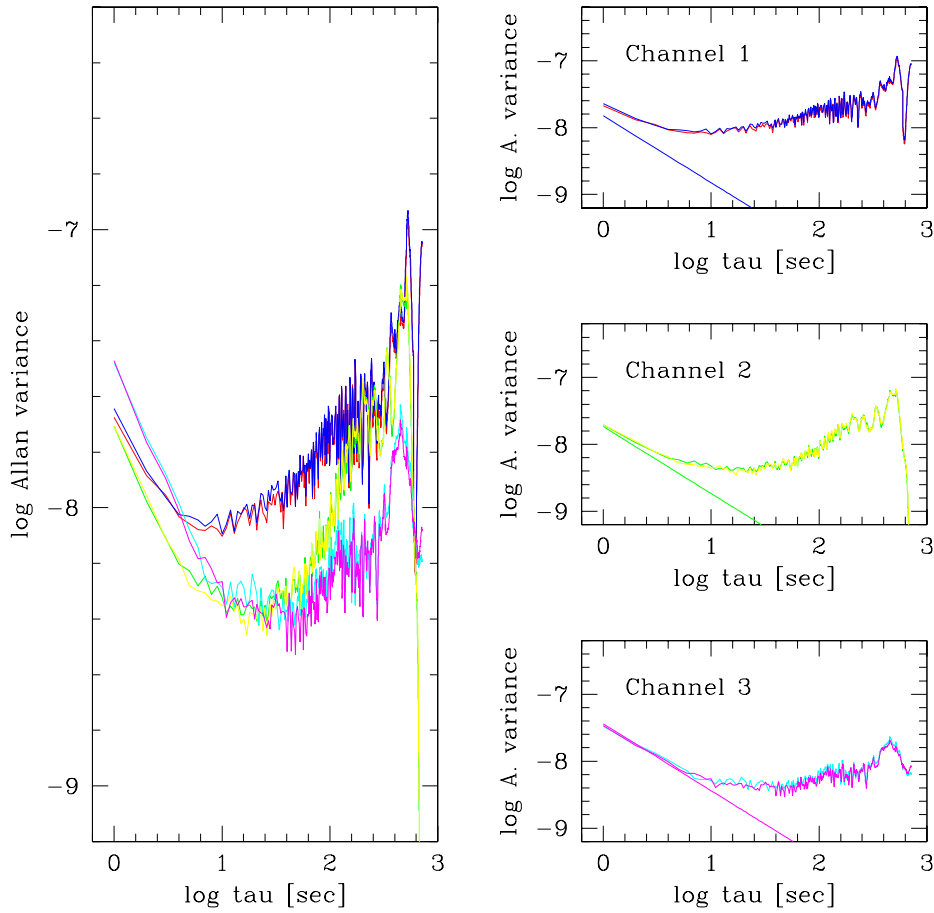


Figure 15. Allan variances of hot and warm loads of channels 1 to 3 for the setup depicted below, also see description for file 008 in table. Channel 1 hot: red, warm: blue. Channel 2 hot: yellow, warm: green. Channel 3 hot: magenta, warm: turquoise. The channel number is defined by the counter, not by the input frequency. The straight lines are the theoretical expectations for thermal noise alone.

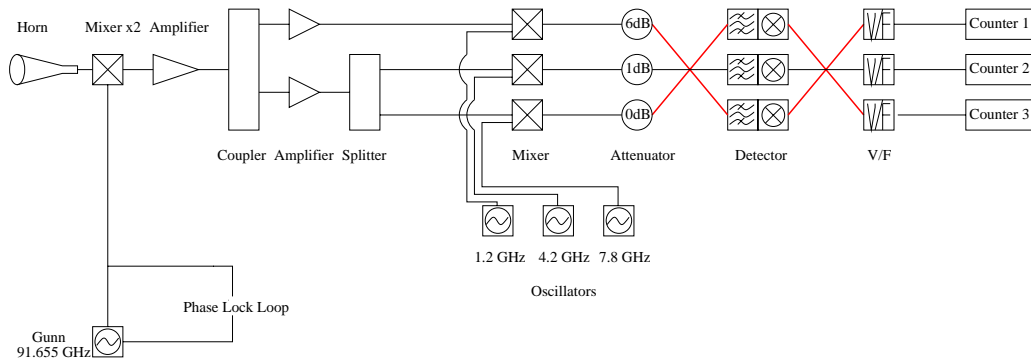


Figure 16. Set-up for Allan variances plotted above (file 008).

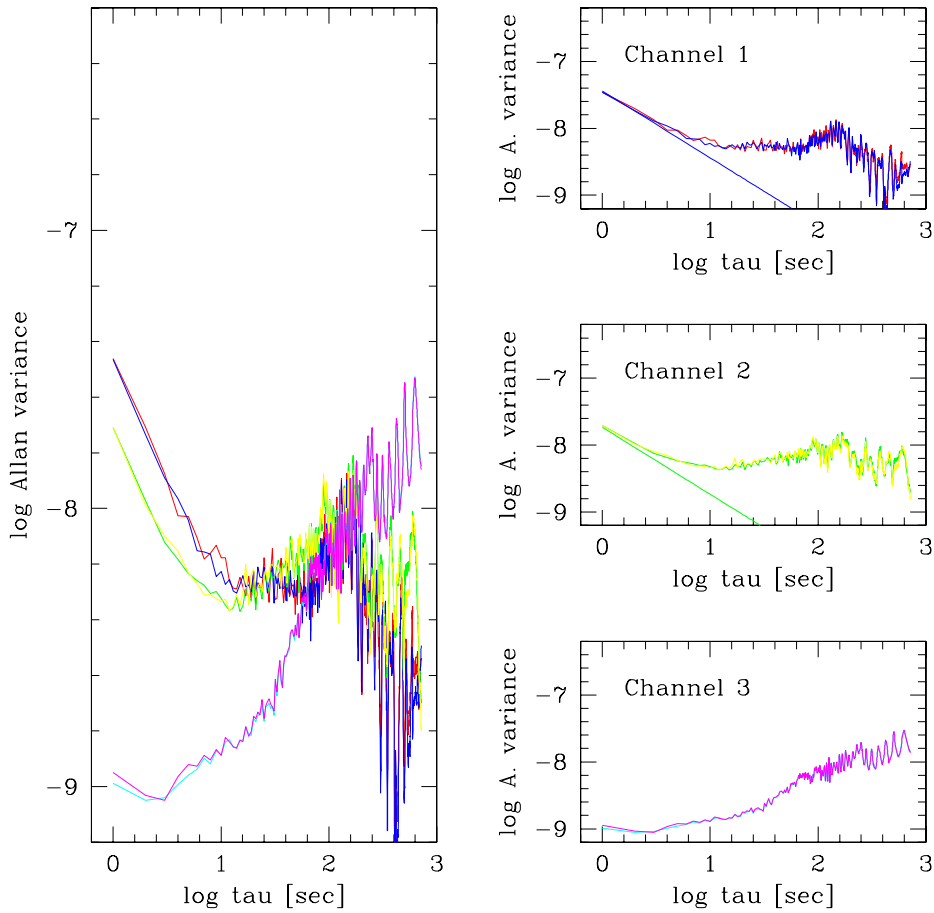


Figure 17. Allan variances of hot and warm loads of channels 1 to 3 for the set-up depicted below, also see description for file 009 in table. Channel 1 hot: red, warm: blue. Channel 2 hot: yellow, warm: green. Channel 3 hot: magenta, warm: turquoise. The straight lines are the theoretical expectations for thermal noise alone.

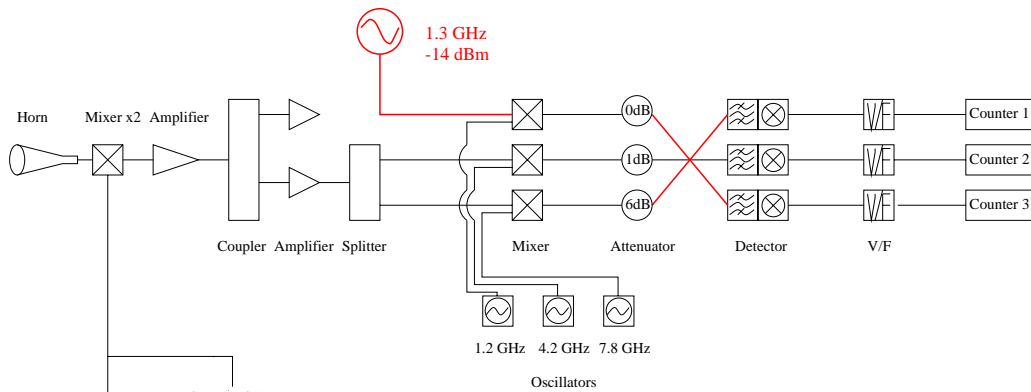


Figure 18. Set-up for Allan variances plotted above (file 009).

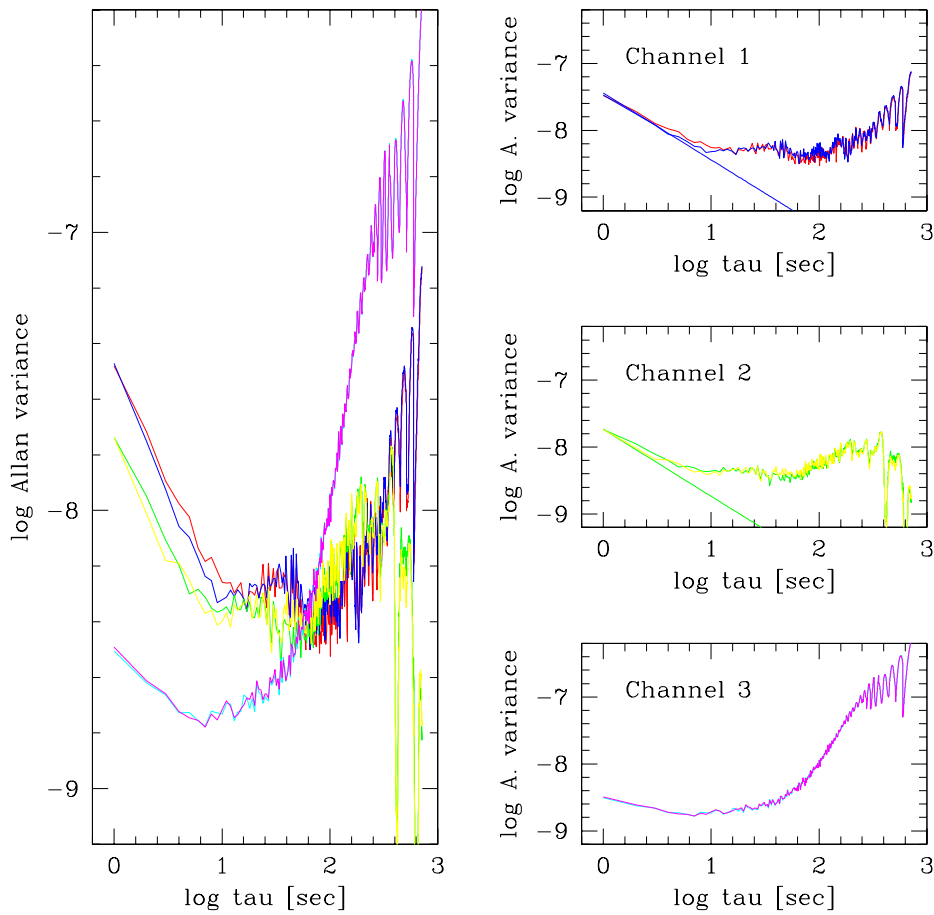


Figure 19. Allan variances of hot and warm loads of channels 1 to 3 for the set-up depicted below, also see description for file 010 in table. Channel 1 hot: red, warm: blue. Channel 2 hot: yellow, warm: green. Channel 3 hot: magenta, warm: turquoise. The straight lines are the theoretical expectations for thermal noise alone.

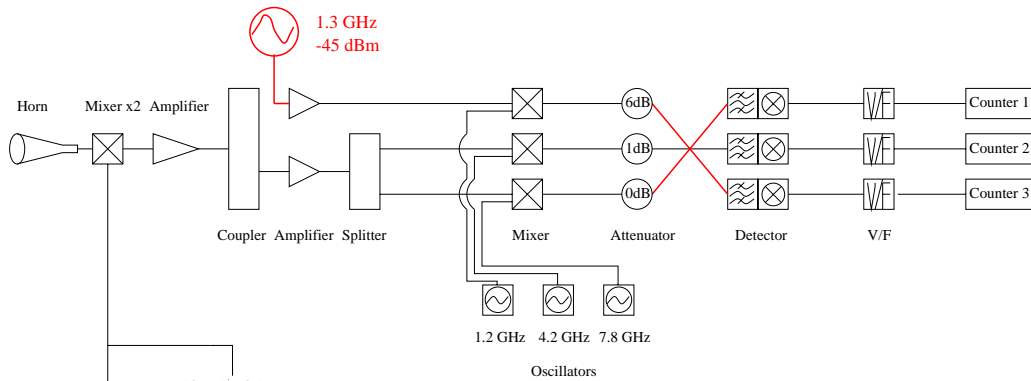


Figure 20. Set-up for Allan variances plotted above (file 010).

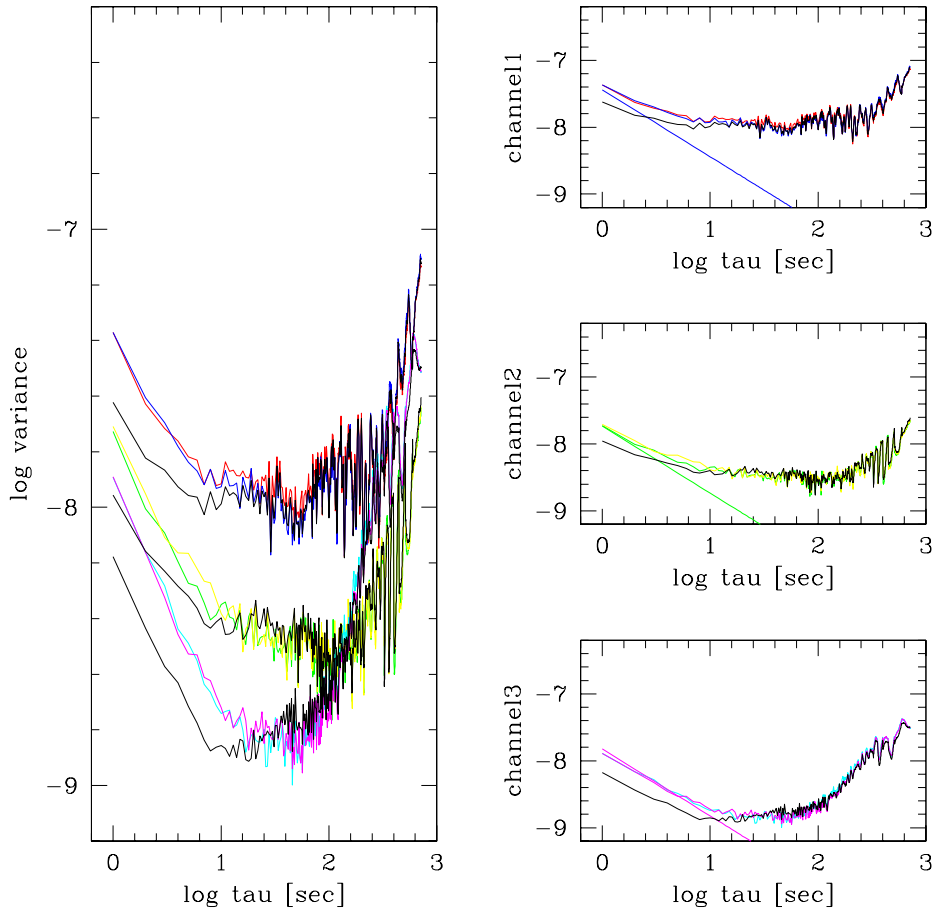


Figure 21. Allan variances of hot and warm loads of channels 1 to 3 for the set-up depicted below. The radiometer was mounted on the CSO telescope which was not moving, also see description for file 019 in table. Channel 1 hot: red, warm: blue, sky: black. Channel 2 hot: yellow, warm: green, sky: black. Channel 3 hot: magenta, warm: turquoise, sky: black. The integration time on the sky is twice as long as on each load.

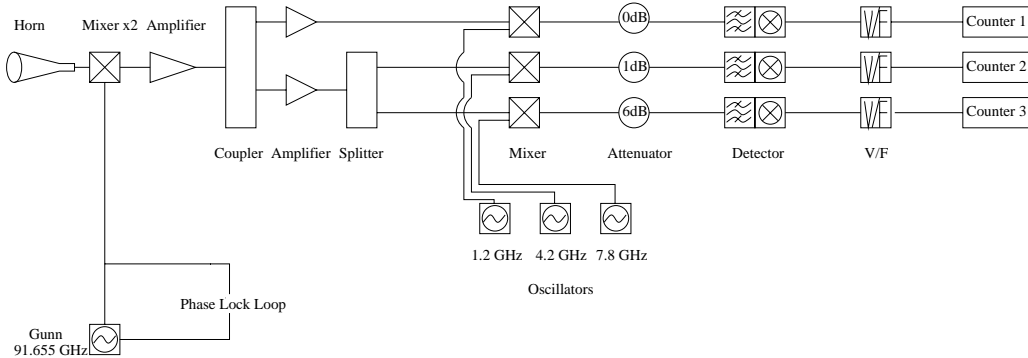


Figure 22. Set-up for Allan variances plotted above (file 019).

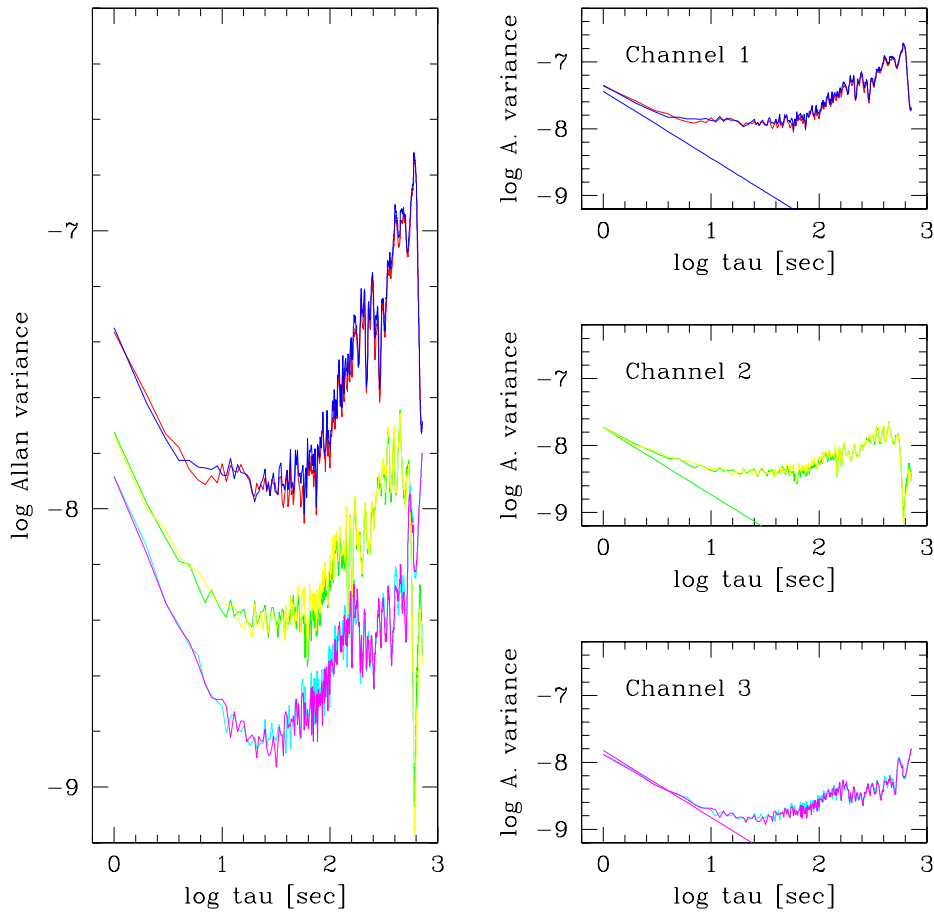


Figure 23. Allan variances of hot and warm loads of channels 1 to 3 for the set-up depicted below. The radiometer was mounted on the CSO looking at the sky. Data was recorded while the telescope was moving. Also see description for file 011 in table. Channel 1 hot: red, warm: blue, sky: black. Channel 2 hot: yellow, warm: green. Channel 3 hot: magenta, warm: turquoise, sky: black. The integration time on the sky is twice as long as on each load.

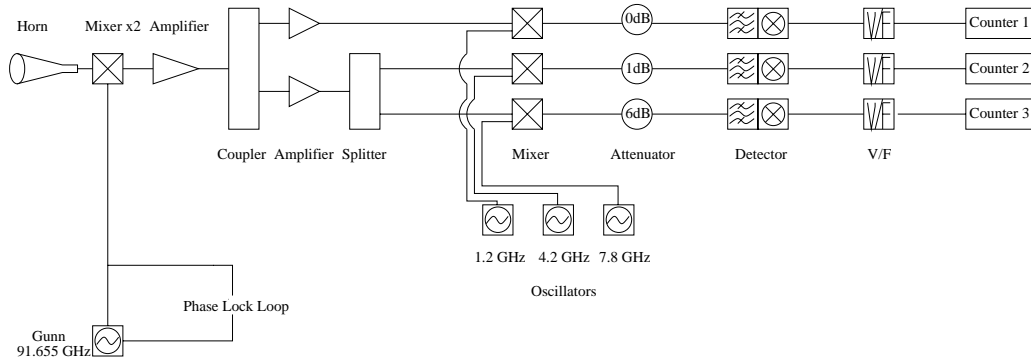


Figure 24. Set-up for Allan variances plotted above (file 011).